

# SEDIMENT TRANSPORT, PART II: SUSPENDED LOAD TRANSPORT

By Leo C. van Rijn<sup>1</sup>

**ABSTRACT:** A method is presented which enables the computation of the suspended load as the depth-integration of the product of the local concentration and flow velocity. The method is based on the computation of the reference concentration from the bed-load transport. Measured concentration profiles have been used for calibration. New relationships are proposed to represent the size-gradation of the bed material and the damping of the turbulence by the sediment particles. A verification analysis using about 800 data shows that about 76% of the predicted values are within 0.5 and 2 times the measured values.

## INTRODUCTION

An essential part of morphological computations in the case of flow conditions with suspended sediment transport is the use of a reference concentration as a bed-boundary condition. At the Delft Hydraulics Laboratory an equilibrium bed concentration has been used so far (24-27). In that approach an equilibrium concentration is computed from the sediment transport capacity as given by a total load transport formula and the relative concentration profile. To improve the bed-boundary condition, a theoretical investigation was initiated at the Delft Hydraulics Laboratory with the aim of determining a relationship which specifies the reference concentration as function of local (near-bed) flow parameters and sediment properties (33,34).

In the present analysis, it will be shown that the function for the bed-load concentration as proposed in Part I, can also be used to compute the reference concentration for the suspended load. Furthermore, the main controlling hydraulic parameters for the suspended load, which are the particle fall velocity and the sediment diffusion coefficient, are studied in detail. Especially investigated and described by new expressions are the diffusion of the sediment particles in relation to the diffusion of fluid particles and the influence of the sediment particles on the turbulence structure (damping effects).

Finally, a method to compute the suspended load transport is proposed and verified, using a large amount of flume and field data.

## CHARACTERISTIC PARAMETERS

In the present analysis it is assumed that the bed-load transport and therefore the reference concentration at the bed are determined by particle parameter  $D_*$  and transport stage parameter  $T$  as

$$D_* = D_{50} \left[ \frac{(s-1)g}{v^2} \right]^{1/3} \dots\dots\dots (1)$$

<sup>1</sup>Proj. Engr., Delft Hydr. Lab., Delft, The Netherlands.

Note.—Discussion open until April 1, 1985. To extend the closing date one month, a written request must be filed with the ASCE Manager of Technical and Professional Publications. The manuscript for this paper was submitted for review and possible publication on October 25, 1982. This paper is part of the *Journal of Hydraulic Engineering*, Vol. 110, No. 11, November, 1984. ©ASCE, ISSN 0733-9429/84/0011-1613/\$01.00. Paper No. 19277.

in which  $D_{50}$  = particle diameter of bed material;  $s$  = specific density;  $g$  = acceleration of gravity; and  $\nu$  = kinematic viscosity coefficient.

$$T = \frac{(u'_*)^2 - (u_{*,cr})^2}{(u_{*,cr})^2} \dots \dots \dots (2)$$

in which  $u'_* = (g^{0.5}/C') \bar{u}$  = bed-shear velocity related to grains;  $C' = 18 \log (12R_b/3D_{90})$  = Chézy-coefficient related to grains;  $R_b$  = hydraulic radius related to the bed according to Vanoni-Brooks (38);  $\bar{u}$  = mean flow velocity; and  $u_{*,cr}$  = critical bed-shear velocity according to Shields (36).

To describe the suspended load transport, a suspension parameter which expresses the influence of the upward turbulent fluid forces and the downward gravitational forces, is defined as

$$Z = \frac{w_s}{\beta \kappa u_*} \dots \dots \dots (3)$$

in which  $w_s$  = particle fall velocity of suspended sediment;  $\beta$  = coefficient related to diffusion of sediment particles;  $\kappa$  = constant of Von Karman; and  $u_*$  = overall bed-shear velocity.

## INITIATION OF SUSPENSION

Before analyzing the main hydraulic parameters which influence the suspended load, it is necessary to determine the flow conditions at which initiation of suspension will occur.

Bagnold stated in 1966 (4) that a particle only remains in suspension when the turbulent eddies have dominant vertical velocity components which exceed the particle fall velocity ( $w_s$ ). Assuming that the vertical velocity component ( $w'$ ) of the eddies are represented by the vertical turbulence intensity ( $\bar{w}$ ), the critical value for initiation of suspension can be expressed as:

$$\bar{w} = [(\overline{w'})^2]^{0.5} \geq w_s \dots \dots \dots (4)$$

Detailed studies on turbulence phenomena in boundary layer flow (20) suggest that the maximum value of the vertical turbulence intensity ( $\bar{w}$ ) is of the same order as the bed-shear velocity ( $u_*$ ). Using these values, the critical bed-shear velocity ( $u_{*,crs}$ ) for initiation of suspension becomes:

$$\frac{u_{*,crs}}{w_s} = 1 \dots \dots \dots (5)$$

which can be expressed as (see Fig. 1)

$$\theta_{crs} = \frac{(u_{*,crs})^2}{(s-1)gD_{50}} = \frac{(w_s)^2}{(s-1)gD_{50}} \dots \dots \dots (6)$$

Another criterion for initiation of suspension has been given by Englund (16). Based on a rather crude stability analysis, he derived:

$$\frac{u_{*,crs}}{w_s} = 0.25 \dots \dots \dots (7)$$

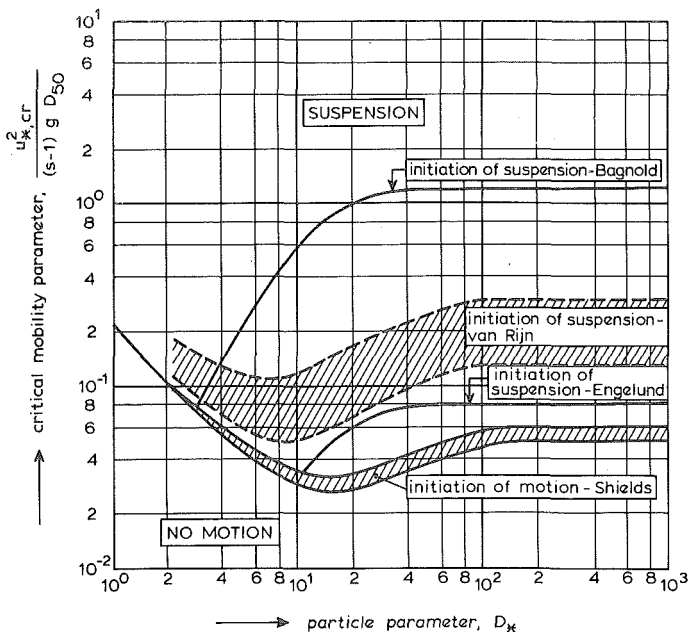


FIG. 1.—Initiation of Motion and Suspension

Finally, some results of experimental research at the Delft Hydraulics Laboratory are reviewed. The writer determined the critical flow conditions at which instantaneous upward turbulent motions of the sediment particles (bursts) with jump lengths of the order of 100 particle diameters were observed (11). The experimental results can be represented by:

$$\frac{u_{*,crs}}{w_s} = \frac{4}{D_*}, \quad \text{for } 1 < D_* \leq 10 \quad \dots \quad (8)$$

$$\frac{u_{*,crs}}{w_s} = 0.4, \quad \text{for } D_* > 10 \quad \dots \quad (9)$$

Eqs. 6–9 are shown in Fig. 1. Summarizing, it is suggested that the criterion of Bagnold may define an upper limit at which a concentration profile starts to develop, while the writer's criterion defines an intermediate stage at which locally turbulent bursts of sediment particles are lifted from the bed into suspension.

## MATHEMATICAL DESCRIPTION OF CONCENTRATION PROFILES

In a steady and uniform flow, the vertical distribution of the sediment concentration profile can be described by:

$$(1 - c) c w_{s,m} + \epsilon_s \frac{dc}{dz} = 0 \quad \dots \quad (10)$$

in which  $c$  = sediment concentration;  $w_{s,m}$  = particle fall velocity in a fluid-sediment mixture;  $\epsilon_s$  = sediment diffusion coefficient; and  $z$  = vertical coordinate.

**Particle Fall Velocity.**—In a clear, still fluid the particle fall velocity ( $w_s$ ) of a *solitary* sand particle smaller than about 100  $\mu\text{m}$  (Stokes-range) can be described by:

$$w_s = \frac{1}{18} \frac{(s-1) g D_s^2}{\nu} \dots\dots\dots (11)$$

For suspended sand particles in the range 100–1,000  $\mu\text{m}$ , the following type of equation, as proposed by Zanke (42), can be used:

$$w_s = 10 \frac{\nu}{D_s} \left\{ \left[ 1 + \frac{0.01 (s-1) g D_s^3}{\nu^2} \right]^{0.5} - 1 \right\} \dots\dots\dots (12)$$

For particles larger than about 1,000  $\mu\text{m}$  the following simple equation can be used (34):

$$w_s = 1.1 [(s-1) g D_s]^{0.5} \dots\dots\dots (13)$$

In Eqs. 11–13 the  $D_s$ -parameter expresses the representative particle diameter of the suspended sediment particles, which may be considerably smaller than  $D_{50}$  of the bed material, as will be shown later on.

Experiments with high sediment concentrations have shown a substantial reduction of the particle fall velocity due to the presence of the surrounding particles. For normal flow conditions with particles in the range 50–500  $\mu\text{m}$  the reduced particle fall velocity can be described by a Richardson-Zaki type equation (34):

$$w_{s,m} = (1-c)^4 w_s \dots\dots\dots (14)$$

**Diffusion Coefficient.**—Usually, the diffusion of fluid momentum ( $\epsilon_f$ ) is described by a parabolic distribution over the flow depth ( $d$ ):

$$\epsilon_f = \frac{z}{d} \left( 1 - \frac{z}{d} \right) \kappa u_* d \dots\dots\dots (15)$$

In the present analysis a parabolic-constant distribution, which means a parabolic distribution in the lower half of the flow depth and a constant value in the upper half of the flow depth, is used mainly because it may give a better description of the concentration profile. The parabolic-constant distribution reads:

$$\epsilon_{f,\max} = 0.25 \kappa u_* d \quad \text{for} \quad \frac{z}{d} \geq 0.5 \dots\dots\dots (16a)$$

$$\epsilon_f = 4 \frac{z}{d} \left( 1 - \frac{z}{d} \right) \epsilon_{f,\max} \quad \text{for} \quad \frac{z}{d} < 0.5 \dots\dots\dots (16b)$$

Eqs. 15 and 16 are shown in Fig. 2. The diffusion of sediment particles ( $\epsilon_s$ ) is related to the diffusion of fluid momentum by:

$$\epsilon_s = \beta \phi \epsilon_f \dots\dots\dots (17)$$

The  $\beta$ -factor describes the difference in the diffusion of a discrete sed-

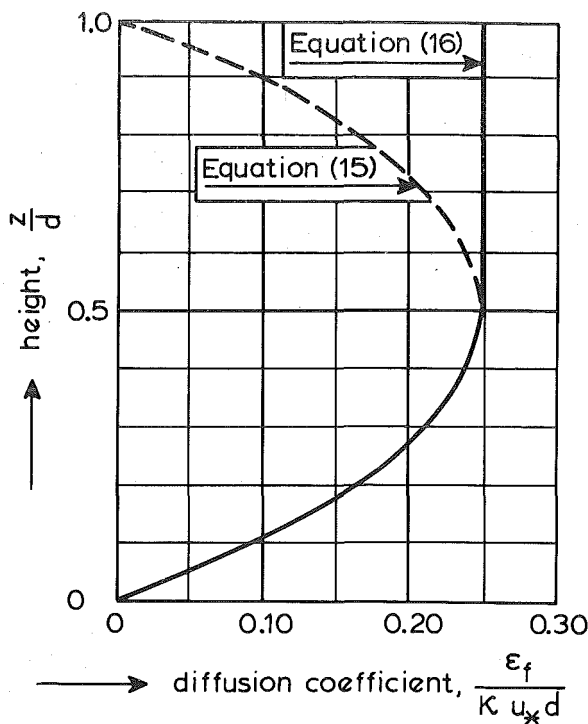


FIG. 2.—Fluid Diffusion Coefficient

iment particle and the diffusion of a fluid “particle” (or small coherent fluid structure) and is assumed to be constant over the flow depth. The  $\phi$ -factor expresses the damping of the fluid turbulence by the sediment particles and is assumed to be dependent on the local sediment concentration. It will be shown (later on) that the  $\beta$ -factor and the  $\phi$ -factor can be described separately.

Firstly, various expressions for the concentration profile will be given.

**Concentration Profiles.**—Using a parabolic-constant  $\epsilon_s$ -distribution according to Eqs. 16 and 17 with  $\phi = 1$  (no damping effect) and a concentration dependent particle fall velocity according to Eq. 14, the sediment concentration profile can be obtained by integration of Eq. 10 resulting in:

$$\sum_{n=1}^4 \left[ \frac{1}{n(1-c)^n} \right] - \sum_{n=1}^4 \left[ \frac{1}{n(1-c_a)^n} \right] + \ln \left[ \frac{(c)(1-c_a)}{(c_a)(1-c)} \right]$$

$$= \ln \left[ \frac{(a)(d-z)}{(z)(d-a)} \right]^z, \quad \text{for } \frac{z}{d} < 0.5 \dots\dots\dots (18a)$$

$$\sum_{n=1}^4 \left[ \frac{1}{n(1-c)^n} \right] - \sum_{n=1}^4 \left[ \frac{1}{n(1-c_a)^n} \right] + \ln \left[ \frac{(c)(1-c_a)}{(c_a)(1-c)} \right]$$

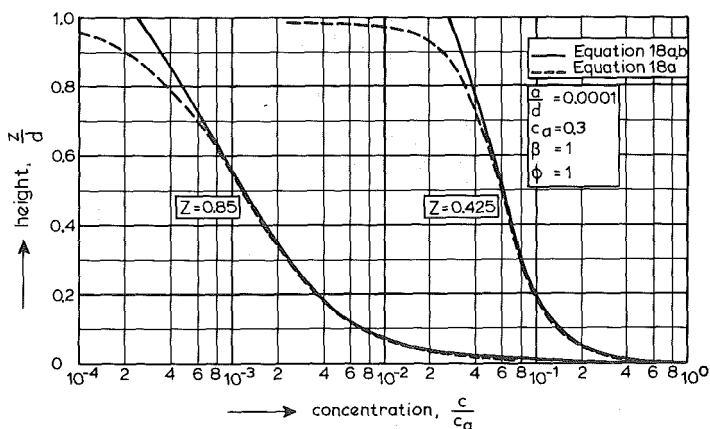


FIG. 3.—Concentration Profiles

$$= -Z \left[ \ln \left( \frac{a}{d-a} \right) + 4 \left( \frac{z}{d} - 0.5 \right) \right], \quad \text{for } \frac{z}{d} \geq 0.5 \dots \dots \dots (18b)$$

in which  $c_a$  = reference concentration;  $a$  = reference level;  $d$  = depth;  $z$  = vertical coordinate; and  $Z$  = suspension parameter. Eqs. 18a–b is shown in Fig. 3. For small concentrations ( $c < c_a < 0.001$ ) Eq. 18a–b reduces to:

$$\frac{c}{c_a} = \left[ \frac{(a)(d-z)}{(z)(d-a)} \right]^Z, \quad \text{for } \frac{z}{d} < 0.5 \dots \dots \dots (19a)$$

$$\frac{c}{c_a} = \left[ \frac{a}{d-a} \right]^Z [e]^{-4Z(z/d-0.5)}, \quad \text{for } \frac{z}{d} \geq 0.5 \dots \dots \dots (19b)$$

Using a parabolic  $\epsilon_s$ -distribution, the concentration profile for the entire flow depth is described by Eq. 18a or 19a, the latter being the well-known Rouse-expression. Eq. 18a is also shown in Fig. 3.

Using a concentration dependent  $\epsilon_s$ -distribution ( $\phi \neq 1$ ), the concentration profile can only be computed by numerical integration of Eq. 10. In the present analysis a simple Runge-Kutta method with an automatic step reduction will be used.

**Influence of Reference Level and Suspension Parameter.**—To show the influence of the reference level ( $a$ ) and the suspension parameter ( $Z$ ) on the concentration profile, Eq. 18a has been solved for  $Z = 1.0, 1.25$  and  $1.5$  (variation of about 20% with respect to the mean value) and a reference level  $a = 0.1d, 0.01d$  and  $0.001d$ . The results are shown in Fig. 4. To simulate increasing sediment concentrations towards the bed, the reference concentration ( $c_a$ ) has been increased from  $c_a = 0.001$  at  $a/d = 0.1$  to  $c_a = 0.1$  at  $a/d = 0.001$  (see Fig. 4).

As can be observed, the concentration profile is relatively sensitive to small variations (about 20%) in the  $Z$ -parameter, particularly for a reference level very close to the bed ( $a = 0.001d$ ). It is evident that a reference level smaller than  $0.01d$  leads to large errors in the concentration profile, but even for  $a = 0.01d$  the prediction of a concentration profile

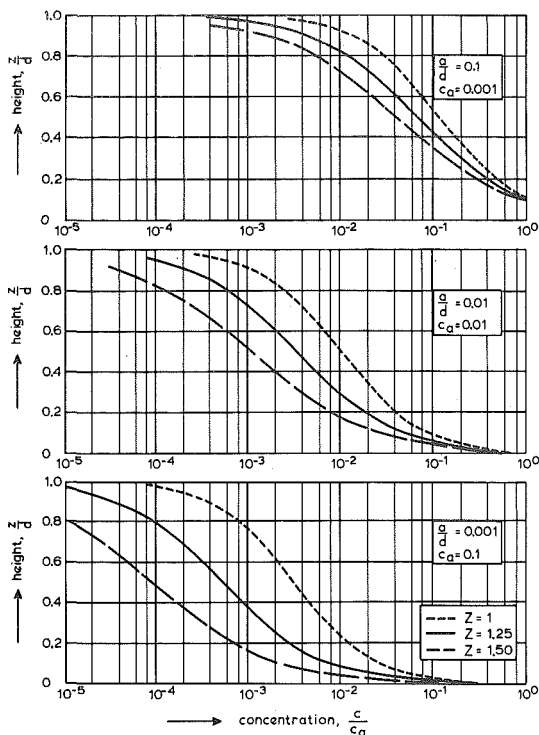


FIG. 4.—Influence of Reference Level and Suspension Parameter

with an error less than a factor 2 requires a  $Z$ -parameter with an error of less than 20% which is hardly possible. Although the particle fall velocity and the bed-shear velocity may be estimated with sufficient accuracy, the accuracy of the  $\beta$ -factor is rather poor.

In this context also the approach of Einstein (12), which is followed by Engelund and Fredsøe (17), is reviewed because he uses a reference level equal to two particle diameters. In the present analysis it has been shown that the approach of Einstein will lead to large errors in the predicted suspended load, because the  $Z$ -parameter cannot be estimated very accurately. Moreover, in the case of flow conditions with bed forms, Einstein's approach is rather artificial. Therefore, the method of Einstein is not attractive to use as a predictive sediment transport theory.

#### INVESTIGATION OF SEDIMENT DIFFUSION COEFFICIENT

**$\beta$ -Factor.**—Some investigators have concluded that  $\beta < 1$  because the sediment particles cannot respond fully to the turbulent velocity fluctuations. Others have reasoned that in a turbulent flow the centrifugal forces on the sediment particles (being of higher density) would be greater than those on the fluid particles, thereby causing the sediment particles to be thrown to the outside of the eddies with a consequent increase in

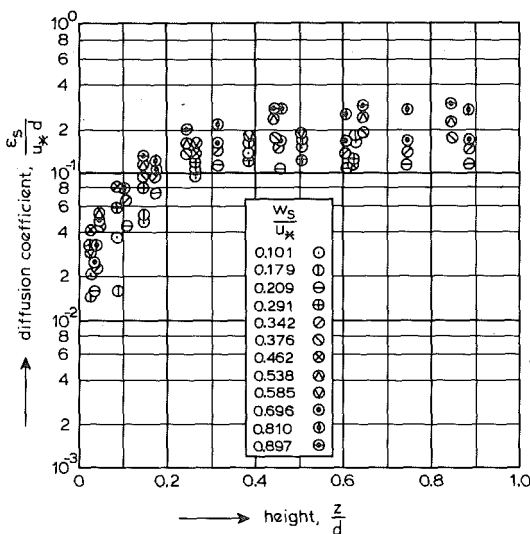


FIG. 5.—Sediment Diffusion Coefficient (Enoree River) According to Coleman

the effective mixing length and diffusion rate, resulting in  $\beta > 1$ . Chien (7) analyzed concentration profiles measured in flume and field conditions. Chien determined the  $Z$ -parameter from the slopes of plotted concentration profiles and compared those values with  $Z = w_s/(\kappa u_*)$ . In most cases the latter (predicted)  $Z$ -values overestimated the  $Z$ -values based on the measurements, thereby clearly indicating  $\beta > 1$ . The results of Chien mainly demonstrate the influence of the  $\beta$ -factor because his results are based on concentrations measured in the upper part of the flow ( $z > 0.1d$ ) where the concentrations are not large enough to cause a significant damping of the turbulence ( $\phi \approx 1$ ). Information about the  $\beta$ -factor in relation to particle characteristics and flow conditions can be obtained from a study carried out by Coleman (9). Coleman computed the  $\epsilon_s$ -coefficient from the following equation:

$$w_s c + \epsilon_s \frac{dc}{dz} = 0 \dots \dots \dots (20)$$

Coleman's results indicate a sediment diffusion coefficient which is nearly constant in the upper half of the flow for each particular value of the ratio  $w_s/u_*$  (see Fig. 5). The writer used the results of Coleman to determine the  $\beta$ -factor, defined as (34):

$$\beta = \frac{\epsilon_{s,\max}}{\epsilon_{f,\max}} = \frac{\epsilon_{s,\max}}{0.25 \kappa u_* d} \dots \dots \dots (21)$$

The maximum value of the  $\epsilon_f$ -distribution is the maximum value according to Eq. 15 for  $z/d = 0.5$ . The  $\epsilon_{s,\max}$ -value was determined as the average value of the  $\epsilon_s$ -values in the upper half of the flow [as given by Coleman (9)], where the concentrations and therefore the damping of



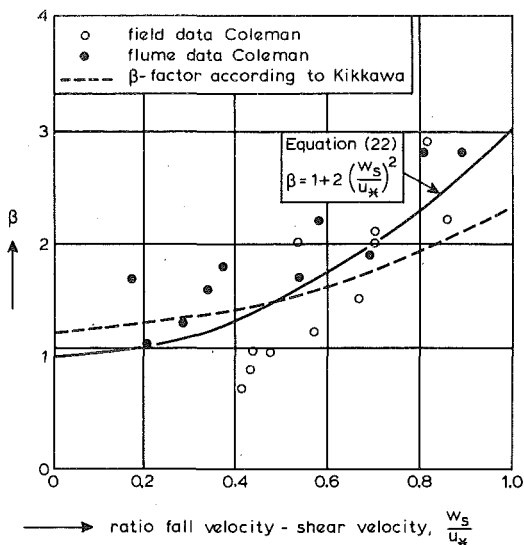


FIG. 6.— $\beta$ -Factor

the turbulence ( $\phi$ -factor) are relatively small. In that way only the influence of the  $\beta$ -factor is considered. The computed  $\beta$ -factors can be described by:

$$\beta = 1 + 2 \left[ \frac{w_s}{u_*} \right]^2, \quad \text{for } 0.1 < \frac{w_s}{u_*} < 1 \dots \dots \dots (22)$$

as shown in Fig. 6. A relationship proposed by Kikkawa and Ishikawa (28), based on a stochastic approach is also shown. According to the present results, the  $\beta$ -factor is always larger than unity, thereby indicating a dominating influence of the centrifugal forces.

**$\phi$ -Factor.**—The  $\phi$ -factor expresses the influence of the sediment particles on the turbulence structure of the fluid (damping effects). Usually the damping effect is taken into account by reducing the constant of Von Karman ( $\kappa$ ). Several investigators have observed that the constant of Von Karman becomes less than the value of 0.4 (clear flow) in the case of a heavy sediment-laden flow over a rigid, flat bed. It has also been observed that the flow velocities in a layer close to the bed are reduced, while in the remaining part of the flow there are larger flow velocities. Apparently, the mixing is reduced by the presence of a large amount of sediment particles. According to Einstein and Chien (13), who determined the amount of energy needed to keep the particles in suspension, the constant of Von Karman is a function of the depth-averaged concentration, the particle fall velocity and the bed-shear velocity.

Although Ippen (23) supposed that the constant of Von Karman is primarily a function of some concentration near the bed, an investigation of Einstein and Abdel-Aal (14) showed only a weak correlation between the near-bed concentration and the constant of Von Karman.

Coleman (10) questioned the influence of the sediment particles on the

constant of Von Karman. Coleman re-analyzed the original data of Einstein-Chien and Vanoni-Brooks and concluded that they used an erroneous method to determine the constant of Von Karman. In view of these contradictions it may be questioned if the concept of an overall constant of Von Karman for the entire velocity profile is correct for a heavy sediment-laden flow. An alternative approach may be the introduction of a local constant of Von Karman ( $\kappa_m$ ) dependent on the local sediment concentration, as has been proposed by Yalin and Finlayson (40). Yalin and Finlayson analyzed measured flow velocity profiles and observed that the local velocity gradient in a sediment-fluid mixture is larger than that in a clear flow. Assuming  $\kappa_m = \phi \kappa$  ( $\phi$  = damping factor for local concentration,  $\kappa = 0.4$ ), Yalin and Finlayson finally derived that:

$$\left(\frac{du}{dz}\right)_m = \frac{1}{\phi} \left(\frac{du}{dz}\right) \dots\dots\dots (23)$$

Using Eq. 23 and flow velocities measured in a flow with and without sediment particles, Yalin and Finlayson determined some  $\phi$ -values, as shown in Fig. 7.

Firstly, it is pointed out that the approach of Yalin and Finlayson is rather simple and based on sometimes rather crude assumptions. Basically, a proper study of the influence of the sediment particles on the velocity and concentration profile requires the solution of the equations of motion and continuity applying a first order closure (mixing length) or a second order (turbulence energy and dissipation) closure. However, as such an approach is far beyond the scope of the present analysis, the writer has modified the approach of Yalin and Finlayson to get a first understanding of the phenomena involved. The modified method is based on the numerical computation of the flow velocity and concentration profile, as (34):

**Velocity Profile.**—Using the hypothesis of Boussinesq, the flow velocity profile in a fluid-sediment mixture is described by:

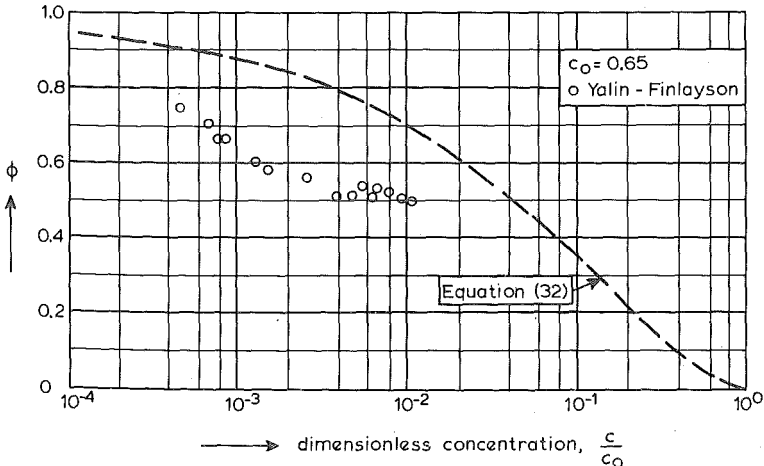


FIG. 7.— $\phi$ -Factor

$$\tau_m = \rho_m (\epsilon_m + \nu_m) \left( \frac{du}{dz} \right)_m \dots \dots \dots (24)$$

in which  $\tau_m$  = shear stress in a fluid-sediment mixture;  $\rho_m$  = local density of mixture;  $\epsilon_m$  = diffusion coefficient of mixture; and  $\nu_m$  = viscosity coefficient of mixture.

Taking  $\tau_m = (1 - z/d) \bar{\rho}_m u_*^2$ , in which  $\bar{\rho}_m$  = average density of mixture and assuming  $\bar{\rho}_m \approx \rho_m$ , the velocity gradient can be expressed as:

$$\left( \frac{du}{dz} \right)_m = \frac{\left( 1 - \frac{z}{d} \right) u_*^2}{\epsilon_m + \nu_m} \dots \dots \dots (25)$$

The diffusion coefficient for the fluid phase of the mixture ( $\epsilon_m$ ) is described by:

$$\epsilon_m = \phi \epsilon_f \dots \dots \dots (26)$$

$$\epsilon_f = 4 \frac{z}{d} \left( 1 - \frac{z}{d} \right) \epsilon_{f,\max} \dots \dots \dots (27)$$

$$\epsilon_{f,\max} = 0.25 \kappa u_* d \dots \dots \dots (28)$$

The  $\phi$ -factor, which has been used as (free) fit-parameter, is supposed to depend on the local concentration and is described by a simple function:

$$\phi = F \left( \frac{c}{c_0} \right) \dots \dots \dots (29)$$

in which  $c$  = local volumetric concentration; and  $c_0 = 0.65$  = maximum volumetric bed concentration.

In a sediment-laden flow, the viscosity coefficient is also modified. Based on experiments with large concentrations, Bagnold (3) derived:

$$\nu_m = \nu (1 + \lambda) (1 + 0.5 \lambda) \dots \dots \dots (30)$$

in which  $\lambda = [(0.74/c)^{1/3} - 1]^{-1}$  = dimensionless concentration parameter.

**Sediment Concentration Profile.**—To describe the concentration profile, Eqs. 10 and 14 are supposed to be valid, resulting in:

$$\frac{dc}{dz} = \frac{w_s c (1 - c)^5}{\epsilon_s} \dots \dots \dots (31)$$

in which  $\epsilon_s = \beta \phi \epsilon_f$  = diffusion coefficient for the sediment phase of the mixture.

The  $\beta$ -factor according to Eq. 22 is assumed to be valid, while the  $\phi$ -factor, as stated before, has been used as a fit-parameter to reproduce measured concentration profiles.

**Determination of  $\phi$ -Factor.**—Three sets of data were used to fit the  $\phi$ -function: (1) The data of Einstein and Chien (13) who measured flow velocity and concentration profiles in a heavy sediment laden flow; (2) the data of Barton and Lin (5); and (3) the data of Vanoni and Brooks

(38). By assuming a  $\phi$ -function and then solving Eqs. 25 and 31 simultaneously by numerical integration and fitting with measured velocity and concentration profiles, the actual  $\phi$ -function was determined. The boundary conditions for the velocity and concentration profiles were:  $u = 0$  at  $z = 0$  and  $c = c_a$  at  $z = a$ , the latter being the concentration ( $c_a$ ) measured in the lowest sampling point ( $a$ ).

Several  $\phi$ -functions were used, but the "best" agreement with measured concentration profiles was obtained by using:

$$\phi = 1 + \left[ \frac{c}{c_0} \right]^{0.8} - 2 \left[ \frac{c}{c_0} \right]^{0.4} \dots\dots\dots (32)$$

Eq. 32, shown in Fig. 7, gives values which are considerably larger (less damping) than those given by Yalin and Finlayson.

Firstly, the results for the experiments of Einstein and Chien are reviewed in more detail. Fig. 8 shows measured and computed results on Run S-15 with the 275  $\mu$ m-sediment. It is remarked that the applied reference concentration was assumed to be equal to the concentration measured in the lowest sampling point, resulting in  $c_a = 625,000$  ppm (by weight) at  $a = 0.005$  m.

The computed concentration and velocity profiles are based on the numerical integration of Eqs. 25 and 31 applying a  $\phi$ -factor according to Eq. 32.

As can be observed, the applied  $\phi$ -function does not give optimal agreement for the entire profile, probably because Eq. 32 is somewhat too simple. Using  $\phi = 1$  (no damping effect) results in computed concentrations which are an order of magnitude larger than the measured values.

As regards the flow velocity profile, the computed velocities are only

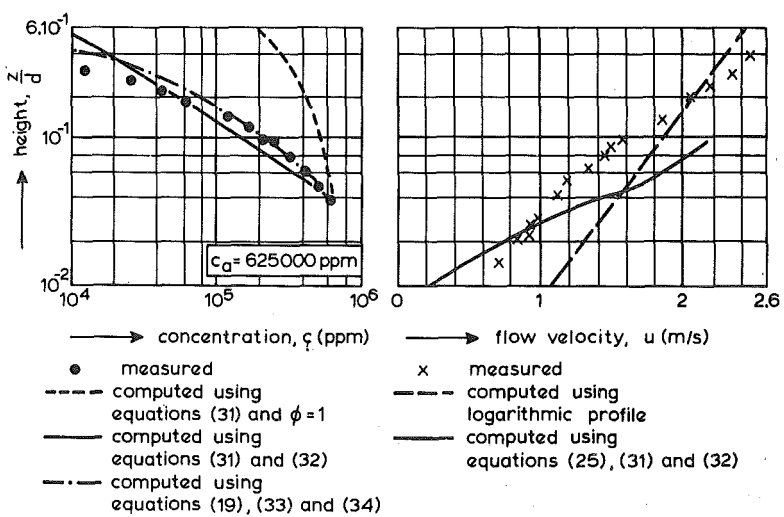


FIG. 8.—Measured and Computed Concentration and Flow Velocity Profiles for Einstein-Chien Experiment (Run S-15)

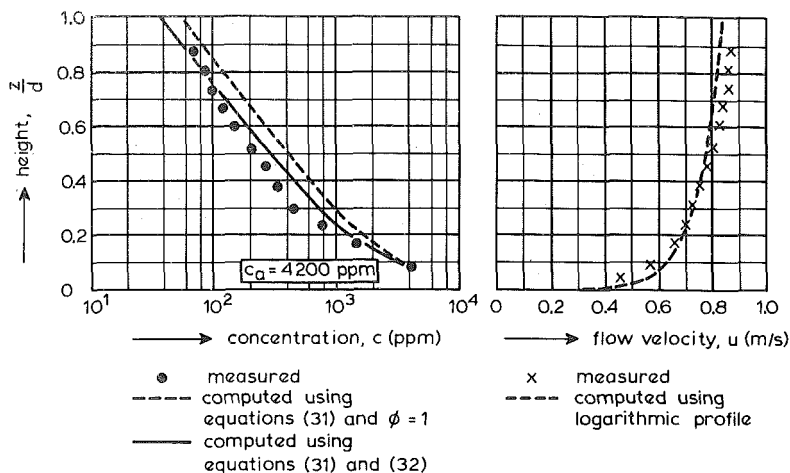


FIG. 9.—Measured and Computed Concentration and Flow Velocity Profiles for Barton-Lin Experiment (Run 31)

of importance in a qualitative sense because the equation of continuity for the fluid has not been taken into account. However, the qualitative trend with reduced flow velocities in the near-bed region is reproduced to some extent. For comparison also the flow velocity profile for a clear flow (Eq. 40) is shown (based on overall flow parameters). Fig. 9 shows measured and computed velocity and concentration profiles for an experiment of Barton and Lin (5) with 180  $\mu\text{m}$ -sediment. It may be noted that the concentrations measured by Barton and Lin are considerably smaller than those in the experiments of Einstein and Chien. Finally, an experiment of Vanoni and Brooks (38) is shown in Fig. 10. For the latter two experiments the flow velocity profile based on Eqs. 25, 31 and 32 is not shown because the computed values were close to the values according to the logarithmic profile.

**Simplified Method.**—The present method is not very suitable for practical use because the concentration profile can only be computed by means of numerical integration of Eq. 31. Therefore, a simplified method based on Eq. 19 in combination with a modified suspension number ( $Z'$ ), is introduced. The modified suspension number ( $Z'$ ) is defined as:

$$Z' = Z + \phi \quad \dots\dots\dots (33)$$

in which  $Z$  = suspension number according to Eq. 3; and  $\phi$  = overall correction factor representing all additional effects (volume occupied by particles, reduction of particle fall velocity and damping of turbulence). The  $\phi$ -values have been determined by means of a trial and error method which implies the numerical computation of concentration profiles (Eqs. 31 and 32) for various sets of hydraulic conditions and the determination of the  $\phi$ -value that yields a concentration profile (Eqs. 19 and 33) similar to the concentration profile based on the numerical method. Therefore for each set of hydraulic conditions ( $w_s, u_*, c_d$ ) a  $\phi$ -value is obtained. Analysis of the  $\phi$ -values showed a simple relationship with the main

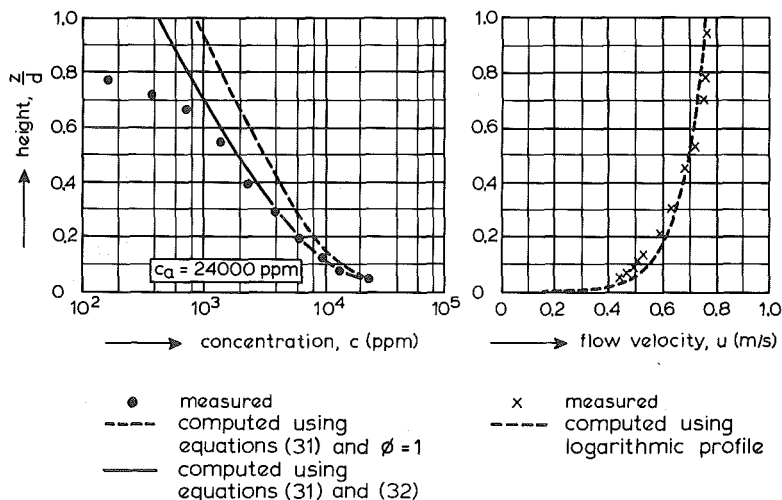


FIG. 10.—Measured and Computed Concentration and Flow Velocity Profiles for Vanoni-Brooks Experiment (Run 3)

hydraulic parameters, as follows (inaccuracy of about 25%):

$$\phi = 2.5 \left[ \frac{w_s}{u_*} \right]^{0.8} \left[ \frac{c_a}{c_0} \right]^{0.4} \quad \text{for} \quad 0.01 \leq \frac{w_s}{u_*} \leq 1 \dots\dots\dots (34)$$

Fig. 8 shows an example of a concentration profile according to the simplified method (Eqs. 1g, 33 and 34).

Summarizing, it is stated that for concentrations larger than about 0.001 ( $\approx 2,500$  ppm) the  $\phi$ -factor becomes smaller than about 0.9 (Fig. 7) and therefore the reduction of the sediment diffusion coefficient must be taken into account. Compared with the concentration profile, the influence of the damping of the turbulence on the velocity profile is relatively small. As stated before, the present analysis only provides a first understanding of the phenomena involved. More research is necessary applying the complete set of equations to compute the concentration and velocity profiles.

**Influence of Bed Forms.**—In a qualitative sense the experiments of Ikeda (22) provide some information about the influence of the bed forms on the concentration profile. Ikeda carried out an experiment with a rigid flat bed in which the amount of sediment particles ( $D_{50} = 180 \mu\text{m}$ ) was controlled so as not to yield deposition and a similar experiment with a movable bed surface. In both experiments the flow conditions were about the same ( $w_s/u_* \approx 0.6$ ), but the concentration profiles in the movable bed experiment were much more uniform than those in the rigid flat bed experiment, thereby indicating a more intensive mixing process due to the bed forms. The computed  $\beta$ -factor was about 2.4 for the movable bed experiment and about 1.3–1.8 for the flat bed experiment. Another remarkable phenomenon observed by Ikeda was the increase of the sediment concentrations by a factor of 10 as the bed forms became three-

dimensional, whereas the bed-shear velocity remained nearly constant.

As regards the influence of the bed forms on the concentration profile, and hence on the suspended load, also the approach of Einstein (12) should be mentioned. Einstein assumed that the diffusion coefficient depends on the bed-shear velocity related to grain-roughness ( $u_*'$ ) instead of the overall bed-shear velocity ( $u_*$ ), which is stated on pages 9 and 25 of his original report (12). The approach of Einstein is remarkable because the diffusion of sediment particles in the main part of the flow is merely related to the overall bed-shear velocity in which the turbulence energy generated in the separated flow regions downstream of the top of the bed forms plays an essential role. Therefore the concept of Einstein, which is followed by Engelund and Fredsøe (17), must be rejected.

Finally, it is stated that for most practical situations the present knowledge of the sediment transport is sufficient to do morphological predictions. However, from a scientific point of view further theoretical and experimental research is necessary to extend the knowledge of the sediment diffusivity ( $\beta$ - and  $\phi$ -factor), while also the influence of the bed forms on the vertical distribution of the fluid diffusivity and therefore the sediment diffusivity must be studied.

## COMPUTATION OF SUSPENDED LOAD

**Reference Concentration.**—In Part I (Bed-Load Transport) a function for the bed-load concentration has been proposed. Generally, however, it is not attractive to use the bed-load concentration as the reference concentration for the concentration profile because it prescribes a concentration at a level equal to the saltation height which may result in large errors for the concentration profile as shown in Fig. 4. Furthermore, this approach is rather artificial in the case of bed forms because the bed-load concentration is an estimate for the concentration in the bed-load layer at the upsloping part of the bed forms. Therefore, another approach (34) is introduced with a reference level ( $a$ ) related to the bed-form height as shown in Fig. 11.

Below the reference level, the transport of all sediment particles is considered as bed-load transport ( $q_b$ ) and an effective reference concentration ( $c_a$ ) is defined as:

$$q_b = c_b u_b \delta_b = c_a \bar{u}_a a \dots \dots \dots (35)$$

in which  $c_b$  = bed-load concentration;  $u_b$  = velocity of bed-load particles;  $\delta_b$  = saltation height;  $\bar{u}_a$  = effective particle velocity; and  $a$  = reference level above bed. Assuming  $\bar{u}_a = \alpha_2 u_b$  and using the proposed relationships (Part I) for the bed-load concentrations ( $c_b$ ) and the saltation height ( $\delta_b$ ), the reference concentration ( $c_a$ ) can be expressed as:

$$c_a = \frac{0.035}{\alpha_2} \frac{D_{50}}{a} \frac{T^{1.5}}{D_*^{0.3}} \dots \dots \dots (36)$$

In the present analysis, the reference level is assumed to be equal to half the bed-form height ( $\Delta$ ), or the equivalent-roughness height ( $k_s$ ) if the bed-form dimensions are not known, while a minimum value  $a = 0.01d$

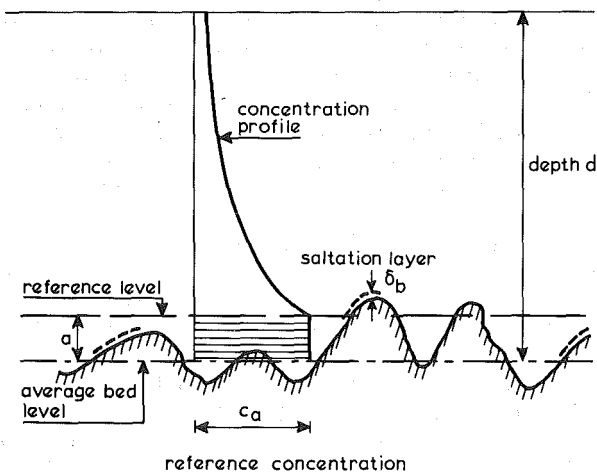


FIG. 11.—Definition Sketch for Reference Concentration

is used for reasons of accuracy (Fig. 4). Thus

$$a = 0.5 \Delta, \text{ or } a = k_s, \text{ (with } a_{\min} = 0.01d) \dots \dots \dots (37)$$

The actual value of the  $\alpha_2$ -factor has been determined by fitting of measured and computed concentration profiles for a range of flow conditions. As only data in the lower flow regime with relatively low concentrations ( $\phi \approx 1$ ) were selected, the concentration profiles were computed using Eqs. 19, 22 and 36. The reference level was assumed to be equal to the equivalent roughness height of Nikuradse, because the bed-form heights were not available for all experiments.

In all, 20 flume and field data were selected, which were the experi-

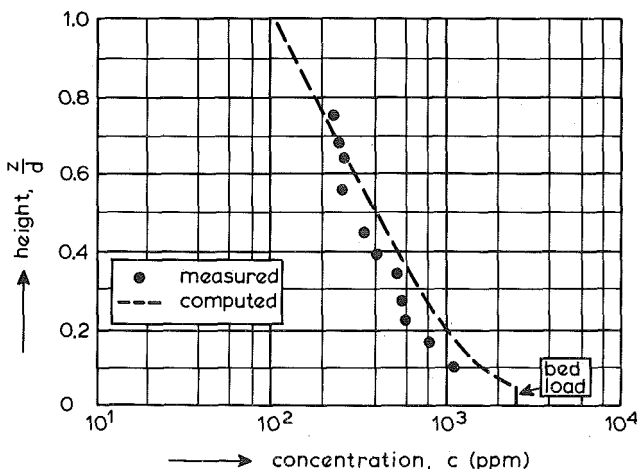


FIG. 12.—Concentration Profile for Barton-Lin Experiment (Run 7)



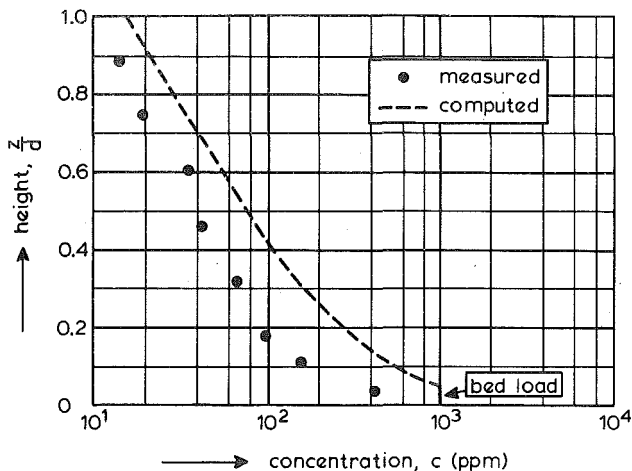


FIG. 13.—Concentration Profile for Enoree River (19 Feb., 1940)

ments of Barton-Lin (5) and concentration profiles measured in the Enoree River (2), in the Mississippi River (35) and an estuary in the Netherlands (Eastern Scheldt). The flow depths varied from 0.1–25 m, the flow velocity varied from 0.4–1.6 m/s and the sediment size from 180–700  $\mu\text{m}$ . The “best” agreement between measured and computed concentration profiles for all data was obtained for  $\alpha_2 = 2.3$  resulting in:

$$c_a = 0.015 \frac{D_{50}}{a} \frac{T^{1.5}}{D_*^{0.3}} \dots \dots \dots (38)$$

Figs. 12, 13, 14 and 15 show some examples of measured and computed

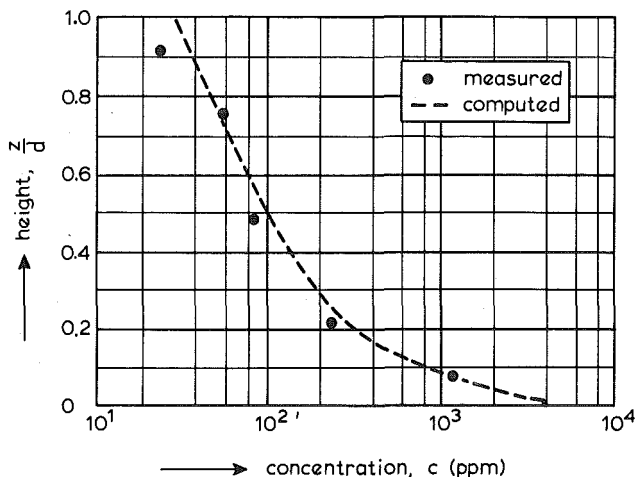


FIG. 14.—Concentration Profile for Mississippi River (station 1100, Apr., 1963)

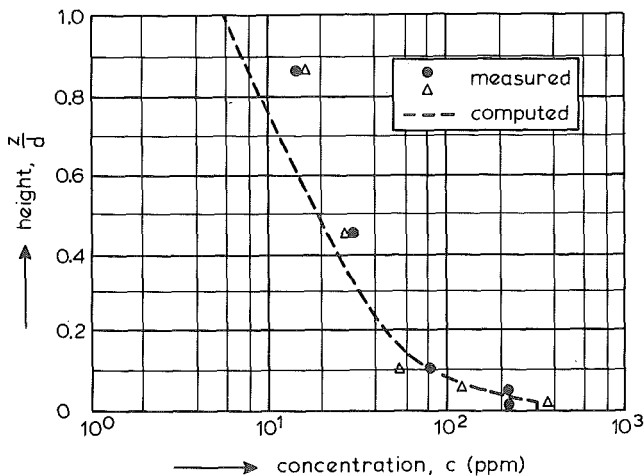


FIG. 15.—Concentration Profile for Eastern Scheldt (Sept., 1978)

concentration profiles for each data set using Eq. 38. In the present state of research the knowledge of the reference concentration is rather limited. Only some graphical results have been presented (18). However, these curves are not well-defined because the reference level is not specified. Therefore, Eq. 38 offers a simple and well-defined expression for the computation of the reference concentration in terms of solids volume per unit fluid volume (or in  $\text{kg}/\text{m}^3$  after multiplying by the sediment density,  $\rho_s$ ).

#### REPRESENTATIVE PARTICLE SIZE OF SUSPENDED SEDIMENT

Observations in flume and field conditions have shown that the sediments transported as bed load and as suspended load have different particle size distributions. Usually, the suspended sediment particles are considerably smaller than the bed-load particles. Basically, it is possible to compute the suspended load for any known type of bed material and flow conditions by dividing the bed material into a number of size fractions and assuming that the size fractions do not influence each other. However, a disadvantage of this method, which has been proposed by Einstein (12), is the relatively large computer costs, particularly for time-dependent morphological computations. Therefore, in the present analysis the Einstein-approach is only used to determine a representative particle diameter ( $D_s$ ) of the suspended sediment (34). Using the size-fractions method, as proposed by Einstein, the total suspended load has been computed for various conditions, after which by trial and error the representative (suspended) particle diameter was determined that gave the same value for the suspended load as according to the size-fractions method. Then, the  $D_s$  parameter has been related to the  $D_{50}$  of the bed material and the  $\sigma_s$  coefficient.

In all, six computations were done using two types of bed material with a geometric standard deviation:  $\sigma_s = 0.5(D_{84}/D_{50} + D_{16}/D_{50}) = 1.5$

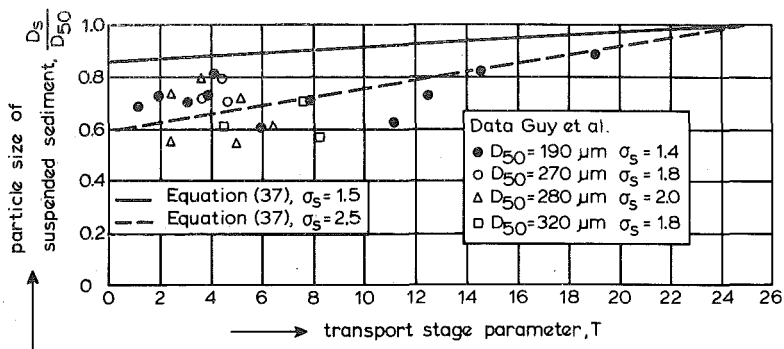


FIG. 16.—Representative Particle Diameter of Suspended Sediment

and 2.5. The  $D_{50}$  of the bed material was equal to 250  $\mu\text{m}$ . The mean flow velocities were 0.5, 1.0 and 1.5 m/s. The flow depth was assumed to be 10 m. The concentration profile was computed by means of Eqs. 19 and 38 with  $\beta = 1$ ,  $\phi = 1$  and  $\kappa = 0.4$ . The reference level was applied at  $a = 0.05d$ . The flow velocity profile was computed according to the logarithmic law for rough flow conditions. The suspended load transport was computed by means of integration over the flow depth of the product of the local concentration and flow velocity. The computational results can be approximated by the following expression:

$$\frac{D_s}{D_{50}} = 1 + 0.011 (\sigma_s - 1)(T - 25) \dots \dots \dots (39)$$

which is shown in Fig. 16 for  $\sigma_s = 1.5$  and 2.5. For comparison, some experimental data given by Guy et al. (19), are also shown. The scatter of the experimental data is too large to detect any influence of the size gradation of the bed material. In an average sense the agreement between the measured values and the computed values for  $\sigma_s = 2.5$  is reasonably good. It may be noted that  $D_s = D_{50}$  for  $T = 25$ . Using the aforementioned approach, a better representation of the suspended load in the case of a graded bed material can be obtained than by taking a fixed particle diameter such as the  $D_{35}$ ,  $D_{50}$  or  $D_{65}$  of the bed material (1,12,15).

**Flow Velocity Profile.**—In a clear fluid with hydraulic rough flow conditions, the flow velocity profile can be described by:

$$\frac{u}{u_*} = \frac{1}{\kappa} \ln \left( \frac{z}{z_0} \right) \dots \dots \dots (40)$$

in which  $z_0 = 0.033 k_s$  = zero-velocity level; and  $k_s$  = equivalent roughness height of Nikuradse.

In the present analysis, it has been shown that Eq. 40 yields an acceptable representation of the flow velocity profile when the sediment load is not too large (Figs. 9 and 10). Therefore, Eq. 40 can be applied to compute the suspended load transport. It must be stressed, however, that for very heavy sediment-laden flows, the application of Eq. 40 may

lead to serious errors in the near-bed region (Fig. 8). Further research is necessary to determine a simple method to compute the velocity profile in the case of heavy sediment-laden flows.

**Suspended Load Transport.**—Usually, the suspended load transport per unit width is computed by integration as:

$$q_s = \int_a^d c u dz \dots\dots\dots (41)$$

Using Eqs. 19, 33, 34 and 40 to describe the concentration profile and the velocity profile, the suspended load transport follows from Eq. 41 resulting in:

$$q_s = \frac{u_* c_a}{\kappa} \left[ \frac{a}{d-a} \right]^{Z'} \left[ \int_a^{0.5d} \left[ \frac{d-z}{z} \right]^{Z'} \ln \left( \frac{z}{z_0} \right) + \int_{0.5d}^d [e]^{-4Z'(z/d-0.5)} \ln \left( \frac{z}{z_0} \right) dz \right] \dots\dots\dots (42)$$

The transport of sediment particles below the reference level ( $a$ ) is considered as bed-load transport (Eq. 35).

Eq. 42 can be represented with an inaccuracy of about 25% by ( $0.3 \leq Z' \leq 3$  and  $0.1 \leq a/d \leq 0.1$ ):

$$q_s = F \bar{u} d c_a \dots\dots\dots (43)$$

$$F = \frac{\left[ \frac{a}{d} \right]^{Z'} - \left[ \frac{a}{d} \right]^{1.2}}{\left[ 1 - \frac{a}{d} \right]^{Z'} [1.2 - Z']} \dots\dots\dots (44)$$

in which  $\bar{u}$  = mean flow velocity;  $d$  = flow depth; and  $c_a$  = reference concentration. The  $F$ -factor is shown for  $a/d = 0.01, 0.05$  and  $0.1$  in Fig. 17.

Summarizing, the complete method to compute the suspended load (volume) per unit width should be applied as:

1. compute particle diameter,  $D_*$  by Eq. 1
2. compute critical bed-shear velocity according to Shields,  $u_{*,cr}$
3. compute transport stage parameter,  $T$  by Eq. 2
4. compute reference level,  $a$  by Eq. 37
5. compute reference concentration,  $c_a$  by Eq. 38
6. compute particle size of suspended sediment,  $D_s$  by Eq. 39
7. compute fall velocity of suspended sediment,  $w_s$  by Eqs. 11, 12 or 13
8. compute  $\beta$ -factor by Eq. 22
9. compute overall bed-shear velocity,  $u_* = (gdS)^{0.5}$
10. compute  $\phi$ -factor by Eq. 34
11. compute suspension parameter  $Z$  and  $Z'$  by Eqs. 3 and 33
12. compute  $F$ -factor by Eq. 44
13. compute suspended load transport,  $q_s$  by Eq. 43

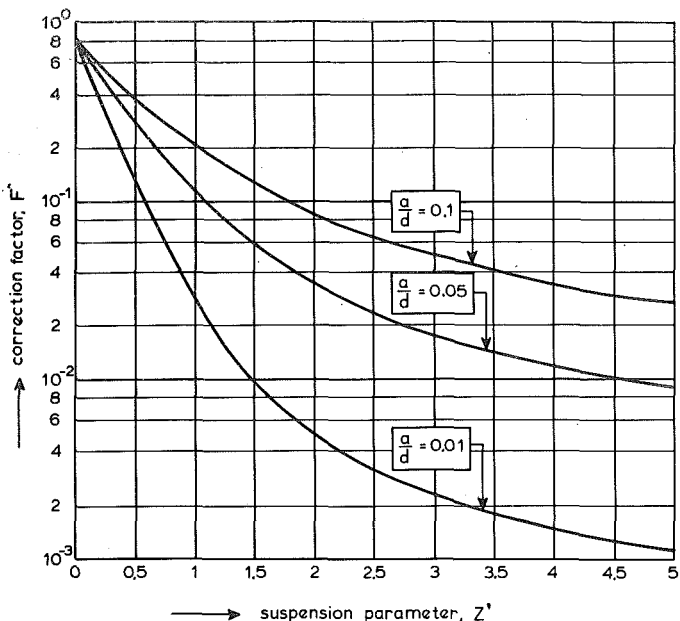


FIG. 17.—F-Factor

The input data are  $\bar{u}$  = mean flow velocity;  $d$  = mean flow depth;  $b$  = mean flow width;  $S$  = energy gradient;  $D_{50}$  and  $D_{90}$  = particle sizes of bed material;  $\sigma_s$  = geometric standard coefficient of bed material;  $\nu$  = kinematic viscosity coefficient;  $\rho_s$  = density of sediment;  $\rho$  = density of fluid;  $g$  = acceleration of gravity; and  $\kappa$  = constant of Von Karman.

#### RATIO OF SUSPENDED LOAD AND TOTAL LOAD

Using Eqs. 35, 43, 44 and  $\varphi = 1$  (low concentrations), the ratio of the suspended and total load transport can be computed as:

$$\frac{q_s}{q_t} = \frac{q_s}{q_s + q_b} = \frac{1}{1 + \left[ \frac{q_b}{q_s} \right]} = \frac{1}{1 + \left[ \frac{1}{F} \frac{\bar{u}_a}{\bar{u}} \frac{a}{d} \right]} \dots \dots \dots (45)$$

The ratio  $\bar{u}_a/\bar{u}$  may be identified as the ratio of the average transport velocity of the bed load and suspended load particles, which varies from about 0.4 for large, steep bed forms in the lower flow regime to about 0.8 for flat bed conditions in the upper flow regime. Fig. 18 shows the ratio of the suspended load and the total load as a function of the ratio of the bed-shear velocity and particle fall velocity for different values of  $\bar{u}_a/\bar{u}$  and  $\beta$ , (with  $\kappa = 0.4$  and  $a/d = 0.5$ ). Also an empirical relationship given by Laursen (29) and some data of Guy et al. (19) are shown. The  $\beta$ -factor must be known to determine the suspension parameter ( $Z$ ) and hence the correction factor ( $F$ ). Two  $\beta$ -functions are applied:  $\beta$  according

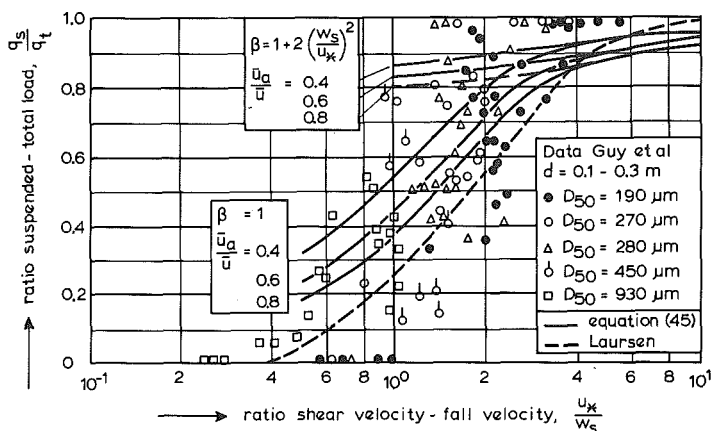


FIG. 18.—Ratio of Suspended Load and Total Load

to Eq. 22 and  $\beta = 1$ . Using Eq. 22, the computed transport ( $q_s/q_t$ ) ratio is much too large compared with the experimental data. Using  $\beta = 1$ , the agreement between computed and measured values is much better, although the experimental data show that for small  $u_*/w_s$ -values the computed transport ratio is still somewhat too large which may be an indication that for small  $u_*/w_s$ -values the sediment diffusivity ( $\epsilon_s$ ) may be relatively small compared with the fluid diffusivity ( $\epsilon_f$ ) and therefore  $\beta < 1$ . Ultimately, the  $\beta$ -factor may approach zero ( $\beta \downarrow 0$ ) for decreasing  $u_*/w_s$ -values. From these results it can be concluded that Eq. 22, which predicts an opposite trend with an increasing  $\beta$ -factor (up to  $\beta = 3$ ) for decreasing  $u_*/w_s$ -values, is not reliable for small  $u_*/w_s$ -values.

Therefore, in the present stage of knowledge, it is proposed to use Eq. 22 for normal flow conditions ( $u_*/w_s > 2$ ), while for low flow stages just beyond initiation of suspension  $\beta = 1$  should be used.

Further research is necessary to investigate the discrepancies between the computed results based on Eq. 22 and the experimental data of Guy et al. (Fig. 18). It is remarked that Eq. 22 is based on measured concentration profiles in the  $u_*/w_s$ -range from 1–10 only [Coleman (9)]. Experimental research is necessary to determine a general  $\beta$ -function for all flow conditions from initiation of suspension to the upper flow regime.

## VERIFICATION

To verify the proposed method, a comparison of predicted and measured values of the total bed material load has been made. As the present analysis is focussed on the computation of the suspended load transport, only data with particle sizes smaller than about 500  $\mu\text{m}$  ( $D_* < 12$ ) were selected. Other selection criteria were: flow depth larger than 0.1 m, mean flow velocity larger than 0.4 m/s, width-depth ratio larger than 3 and a Froude number smaller than 0.9. Most of the flume and field data (Table 1) were selected from a compendium of Solids Transport

compiled by Peterson and Howells (31). As reported by Brownlie (6), various sets of this data bank contain a number of errors. The data sets used in the present analysis are free of the errors uncovered by Brownlie with exception of the Indian Canal data which contain a 12% error in the sediment concentration. The present writer has eliminated this error before using the data. Therefore, all data used in the present analysis can be considered as reliable data. In addition to the data bank of Peterson and Howells, the writer has used 87 data from the Pakistan Canals (30), 46 data from the Middle Loup River (21) and 57 data from the Niobrara River (8). In all, 486 field data and 297 flume data were used. Firstly, the field data are described in more detail. The USA-River data collected by the Corps of Engineers consist of 30 data from the Rio Grande River near Bernalillo, 65 data from the Atchafalaya River near Simmesport, 45 data from the Mississippi River near Tarbert Landing, 100 data from the Mississippi River near St. Louis and 26 data from the Red River near Alexandria. The USA-River data include the bed material load in the measured zone and the estimated bed material load in the unmeasured zone. The bed material loads of the Indian and Pakistan Canals as used in the present analysis only include the bed material loads in the measured zone and are, therefore, less than the total bed material loads. The data from the Middle Loup River and the Niobrara River represent the total bed material loads. Finally, it is remarked that the wash-load is excluded from all field data and that a water temperature of 15° C has been assumed, if not reported. Where the geometric standard deviation of the bed material was not known, a value of 2 was assumed.

A side-wall correction method according to Vanoni-Brooks (38) has been used to eliminate the side-wall roughness.

The suspended load transport ( $q_s$ ) according to the writer's method is computed from Eq. 43, while the bed-load transport ( $q_b$ ) is computed as given in Part I (October Journal of Hydr. Engrg.). The total load transport is computed as  $q_t = q_s + q_b$ . For comparison also the total load formulas of Engelund-Hansen (15), Ackers-White (1) and Yang (41) were used. The accuracy of the four methods is given in terms of a discrepancy ratio ( $r$ ) defined as:

$$r = \frac{q_{t,\text{computed}}}{q_{t,\text{measured}}} \dots\dots\dots (46)$$

For all data, the score of the predicted values in the ranges  $r = 0.75$ – $1.5$ ,  $0.5$ – $2$  and  $0.33$ – $3$  were determined. The results are given in Table 1. The writer's method yields the best results for the field data and the best results for all data used. This is a remarkably good result particularly when it is remembered that only 20 data were used to calibrate the function for the reference concentration. Analysis of the data showed no systematic errors of the total load in relation to the  $T$ - and  $D_*$ -parameters (34). The method of Yang yields excellent results for the flume data and the small-scale river data (Middle Loup and Niobrara River), but very poor results for large-scale rivers (flow depth larger than 1 m). This cannot be attributed to the quality of the large-scale river data, because the other three methods produce reasonable results for these data sets. Therefore, the method of Yang must have serious systematic errors

TABLE 1.—Comparison of Computed and

Source (1)	Num- ber (2)	Flow velocity, in meters per second (3)	Flow depth, in meters (4)	Particle diameter, micro- meter (5)	Temper- ature, in degrees Celsius (6)
Field data					
Various USA-Rivers (Corps-Engr.)	266	0.4-2.4	0.3-17	120-160	2-35
Middle Loup River	46	0.65-1.15	0.3-0.65	300-400	0-30
India-canal	30	0.7-1.6	1.3-3.4	90-310	10-30
Pakistan canals	87	0.6-1.3	1.4-3.6	110-290	15-35
Niobrara River	57	0.6-1.3	0.4-0.65	280	0-30
	486				
Flume Data					
Guy et al.	90	0.4-1.2	0.1-0.4	190-470	8-34
Oxford	84	0.4-1.3	0.1-0.4	100	14-30
Stein	37	0.4-1.2	0.1-0.4	400	20-30
Southampton A	33	0.4-0.8	0.15-0.3	150	15-25
Southampton B	33	0.4-0.55	0.15	480	21
Barton-Lin	20	0.4-0.95	0.15-0.4	180	15-27
	297				
Total	783				

for large flow depths. On the average, the predicted values are much too small.

As regards the experimental data used for calibration and verification, some remarks are made with respect to the accuracy of the measured values. The writer has analyzed some Laboratory experiments performed under similar flow conditions (34). The results show deviations up to a factor 2. Based on these results, it may be concluded that it seems hardly possible to predict the total load with an inaccuracy of less than a factor 2. The relatively low accuracy of measured transport rates also justifies the use of simple approximation functions with less accuracy to avoid the use of complicated numerical solution methods (Eq. 43).

## CONCLUSIONS

The aim of the present analysis was to determine a relationship which specifies the reference concentration as a function of local (near-bed) flow parameters and sediment properties (Eq. 38) and to investigate the parameters controlling the suspended load transport. From the results of the verification analysis it can be concluded that the proposed relationships have a good predictive ability for a range of flow conditions. Furthermore, the present method gives detailed information about all parameters of importance to the sediment transport process. In the writer's opinion this detailed knowledge of the main controlling parameters is of essential importance for a reliable morphological prediction and,



## Measured Total Load Transport

SCORES (%) OF PREDICTED TOTAL LOAD DISCREPANCY RANGES											
0.75 ≤ r ≤ 1.5				0.5 ≤ r ≤ 2				0.33 ≤ r ≤ 3			
Van Rijn (7)	Engelund-Hansen (8)	Ackers-White (9)	Yang (10)	Van Rijn (11)	E-H (12)	A-W (13)	Yang (14)	Van Rijn (15)	E-H (16)	A-W (17)	Yang (18)
53%	39%	32%	6%	79%	67%	61%	24%	94%	87%	78%	44%
39	13	37	63	78	37	74	94	96	80	98	100
30	15	27	3	60	45	48	6	90	73	70	24
23	37	34	13	56	71	71	29	91	94	91	48
55	13	29	86	95	67	58	98	98	95	98	98
45%	32%	32%	22%	76%	64%	63%	39%	94%	88%	84%	55%
40	67	56	68	70	89	85	90	91	98	99	98
37	20	31	45	84	38	59	89	96	70	81	96
54	73	81	56	70	95	97	97	97	97	100	100
64	49	46	49	85	73	79	82	97	91	94	94
18	12	82	91	81	82	96	97	94	97	100	100
35	60	30	40	65	100	50	65	100	100	100	100
41%	46%	52%	59%	77%	74%	77%	89%	95%	89%	94%	98%
43%	37%	40%	36%	76%	68%	68%	58%	94%	88%	88%	71%

therefore, an important advantage to simple formulas which only produce a number. Summarizing, the study has led to the following conclusions:

1. The proposed function for the reference concentration yields good results for predicting the sediment transport for fine particles in the range 100–500 μm.
2. The ratio of the sediment diffusion coefficient and the fluid diffusion coefficient ( $\beta$ -factor) may be larger than unity, but its value cannot be predicted with high accuracy (Eq. 22).
3. The damping of the turbulence by the sediment particles can be taken into account by a local concentration-dependent damping factor ( $\phi$ -factor Eq. 32).
4. In the case of flow conditions with a graded bed material the representative particle diameter of the suspended sediment can be described as a function of the flow stage parameter, the geometrical standard deviation and median size of the bed material (Eq. 39).
5. The concentration profile is rather sensitive to small variations in the particle fall velocity of the suspended sediment, the bed-shear velocity and the  $\beta$ -factor, particularly for a reference level close to the bed.
6. The total sediment load cannot be predicted with an inaccuracy less than a factor 2 because the accuracy of the main controlling parameters is too low, while also the total load data used for calibration and verification show deviations up to a factor 2.

Finally, some remarks are made with respect to the input data of the

proposed method as well as the methods of Engelund-Hansen, Ackers-White and Yang. In the verification analysis the methods were not really used in a fully predictive sense because the bed-shear velocity was computed from the measured energy or surface gradient. To be really predictive, a sediment transport theory should also comprise a bed-roughness predictor as stated by the Task-committee (39). This topic will be reviewed in Part II (to be published in the Dec. Journal of Hydr. Engrg.).

## ACKNOWLEDGMENT

H. N. C. Breusers and N. J. van Wijngaarden of the Delft Hydraulics Laboratory and M. de Vries of the Delft University of Technology are gratefully acknowledged for their theoretical support.

## APPENDIX I.—REFERENCES

1. Ackers, P., and White, R., "Sediment Transport: New Approach and Analysis," *Journal of the Hydraulics Division*, ASCE, No. HY11, 1973.
2. Anderson, A. G., "Distribution of Suspended Sediment in a Natural Stream," *Transactions, American Geophysical Union, Papers, Hydrology*, 1942.
3. Bagnold, R. A., "Experiments on a Gravity-free Dispersion of Large Solid Spheres in a Newtonian Fluid under Shear," *Proceedings of the Royal Society*, Vol. 225 A, 1954, p. 60.
4. Bagnold, R. A., "An Approach to the Sediment Transport Problem for General Physics," *Geological Survey Professional Paper 422-I*, Washington, D.C., 1966.
5. Barton, J. R., and Lin, P. N., "A Study of the Sediment Transport in Alluvial Streams," *Report No. 55 JRB2*, Civil Engineering Department, Colorado College, Fort Collins, Colo., 1955.
6. Brownlie, W. R., discussion of "Total Load Transport in Alluvial Channels," *Journal of the Hydraulics Division*, ASCE, No. HY12, 1981.
7. Chien, N., "The Present Status of Research on Sediment Transport," *Journal of the Hydraulics Division*, ASCE, Vol. 80, 1954.
8. Colby, B. R., and Hembree, C. H., "Computations of Total Sediment Discharge Niobrara River near Cody, Nebraska," *Geological Survey Water-Supply Paper 1357*, Washington, D.C., 1955.
9. Coleman, N. L., "Flume Studies of the Sediment Transfer Coefficient," *Water Resources*, Vol. 6, No. 3, 1970.
10. Coleman, N. L., "Velocity Profiles with Suspended Sediment," *Journal of Hydraulic Research*, Vol. 19, No. 3, 1980.
11. Delft Hydraulics Laboratory, "Initiation of Motion and Suspension, Development of Concentration Profiles in a Steady, Uniform Flow without Initial Sediment Load," *Report M1531-III*, Delft, The Netherlands, 1982.
12. Einstein, H. A., "The Bed-Load Function for Sediment Transportation in Open Channel Flows," *Technical Bulletin No. 1026*, Department of Agriculture, Washington, D.C., 1950.
13. Einstein, H. A., and Chien, N., "Effects of Heavy Sediment Concentration Near the Bed on Velocity and Sediment Distribution," M.R.D. Sediment Series No. 8, University of California, Berkeley, Calif., 1955.
14. Einstein, H. A., and Abdel-Aal, F. M., "Einstein Bed-Load Function at High Sediment Rate," *Journal of the Hydraulics Division*, ASCE, Vol. 98, No. HY1, 1972.
15. Engelund, F., and Hansen, E., "A Monograph on Sediment Transport in Alluvial Streams," Teknisk Forlag, Copenhagen, Denmark, 1967.
16. Engelund, F., "A Criterion for the Occurrence of Suspended Load," *La Houille Blanche*, No. 8, 1965, p. 7.

17. Engelund, F., and Fredsøe, J., "A Sediment Transport Model for Straight Alluvial Channels," *Nordic Hydrology*, 1976, p. 294.
18. Garde, R. J., and Ranga Raju, K. G., "Mechanics of Sediment Transportation and Alluvial Streams Problems," Wiley Eastern Ltd., 1977, p. 171.
19. Guy, H. P., Simons, D. B., and Richardson, E. V., "Summary of Alluvial Channel Data from Flume Experiments," 1956-1961, *Geological Survey Professional Paper 462-I*, Washington, D.C., 1966.
20. Hinze, J. O., *Turbulence* (second edition), McGraw-Hill Book Co., Inc., New York, N.Y., 1975, pp. 640-645.
21. Hubbell, D. W., and Matejka, D. Q., "Investigations of Sediment Transportation Middle Loup River at Dunning, Nebraska," *Geological Survey Water-Supply Paper 1476*, Washington, D.C., 1959.
22. Ikeda, S., "Suspended Sediment on Sand Ripples," Third International Symposium on Stochastic Hydraulics, Tokyo, Japan, 1980.
23. Ippen, A. F., "A New Look at Sedimentation in Turbulent Streams," *Journal of the Boston Society of Civil Engineers*, Vol. 58, No. 3, 1971.
24. Kerssens, P. J. M., "Adjustment Length of Suspended Sediment Profiles (in Dutch), River Engineering Department, Delft Technical University, The Netherlands, 1974.
25. Kerssens, P. J. M., and Rijn, L. C. van, "Model for Non-steady Suspended Transport," Seventeenth Congress IAHR, Baden-Baden, West Germany, Publication No. 91, Delft Hydraulics Laboratory, Delft, The Netherlands, 1977.
26. Kerssens, P. J. M., "Morphological Computations for Suspended Sediment Transport," *Report S78-VI*, Delft Hydraulics Laboratory, Delft, The Netherlands, 1978.
27. Kerssens, P. J. M., Prins, A., and Rijn, L. C. van, "Model for Suspended Sediment Transport," *Journal of the Hydraulics Division*, ASCE, No. HY5, 1979.
28. Kikkawa, H., and Ishikawa, K., "Applications of Stochastic Processes in Sediment Transport," Water Resources Publications, M. Hino, ed., Littleton, Colo., 1980, pp. 8-22.
29. Laursen, E. M., "The Total Sediment Load of Streams," *Journal of the Hydraulics Division*, ASCE, No. HY1, 1958.
30. Mahmood, K., "Selected Equilibrium State Data from ACOP Canals," Civil Mechanical Environmental Engineering Department, George Washington University, *Report No. EWR-79-2*, Washington, D.C., 1972.
31. Peterson, A. W., and Howells, R. F., "A Compendium of Solids Transport Data for Mobile Boundary Channels," *Report No. HY-1973-ST3*, Department of Civil Engineering, University of Alberta, Canada, 1973.
32. Rijn, L. C., van., "Model for Sedimentation Predictions," Nineteenth Congress IAHR, New Delhi, India, Publication No. 241, Delft Hydraulics Laboratory, Delft, The Netherlands, 1981.
33. Rijn, L. C. van, "Computation of Bed-Load Concentration and Transport," *Report S487-I*, Delft Hydraulics Laboratory, Delft, The Netherlands, 1981.
34. Rijn, L. C. van, "Computation of Bed-Load and Suspended Load," *Report S487-II*, Delft Hydraulics Laboratory, Delft, The Netherlands, 1982.
35. Scott, C. H., and Stephens, H. D., "Special Sediment Investigations Mississippi River at St. Louis, Missouri, 1961-1963," *Geological Survey Water Supply Paper 1819-J*, Washington, D.C., 1966.
36. Shields, A., Anwendung der Ähnlichkeitsmechanik und der Turbulenz Forschung auf die Geschiebe Bewegung, Mitt. der Preuss. Versuchsanst. für Wasserbau und Schiffbau, Heft 26, Berlin, Germany, 1936.
37. Subcommittee on Sedimentation, Inter-Agency Committee on Water Research, *Report No. 12*, Minneapolis, Minn., 1957.
38. Vanoni, V. A., and Brooks, N. H., "Laboratory Studies of the Roughness and Suspended Load of Alluvial Streams," Sedimentation Laboratory, California Institute of Technology, *Report E-68*, Pasadena, Calif., 1957.
39. Task Committee, "Sediment Transportation Mechanics: Hydraulic Relations for Alluvial Streams," *Journal of the Hydraulics Division*, ASCE, No. HY1, 1971.
40. Yalin, M. S., and Finlayson, G. D., "On the Velocity Distribution of the Flow-

- carrying Sediment in Suspension," Symposium to Honour Professor H. A. Einstein, H. W. Shen, ed., 1972, pp. 8-11.
41. Yang, C. T., "Incipient Motion and Sediment Transport," *Journal of the Hydraulics Division*, ASCE, Vol. 99, No. HY10, Oct., 1973.
  42. Zanke, U., Berechnung der Sinkgeschwindigkeiten von Sedimenten, Mitt. des Franzius-Instituts für Wasserbau, Heft 46, Seite 243, Technical University, Hannover, West Deutschland, 1977.

## APPENDIX II.—NOTATION

The following symbols are used in this paper:

- $a$  = reference level, (L);
- $C$  = overall Chézy coefficient, ( $L^{0.5} T^{-1}$ );
- $C'$  = Chézy coefficient related to grains, ( $L^{0.5} T^{-1}$ );
- $c$  = concentration (volume =  $\rho_s 10^3 c$  in ppm);
- $c_a$  = reference concentration;
- $c_b$  = bed-load concentration;
- $c_0$  = maximum (bed) concentration (= 0.65);
- $D_*$  = particle parameter;
- $D_{50}$  = particle diameter of bed material, (L);
- $D_s$  = representative particle diameter of suspended sediment, (L);
- $d$  = flow depth, (L);
- $F$  = correction factor for suspended load;
- $g$  = acceleration of gravity, ( $L T^{-2}$ );
- $k_s$  = equivalent roughness height of Nikuradse, (L);
- $q_b$  = bed-load transport per unit width, ( $L^3 T^{-1}$ );
- $q_s$  = suspended load transport per unit width, ( $L^3 T^{-1}$ );
- $q_t$  = total load transport per width, ( $L^3 T^{-1}$ );
- $R_b$  = hydraulic radius of the bed, (L);
- $R$  = Reynolds' number;
- $r$  = discrepancy ratio;
- $S$  = slope;
- $s$  = specific density;
- $T$  = transport stage parameter;
- $Te$  = temperature, ( $^{\circ}C$ );
- $u$  = local mean longitudinal flow velocity, ( $L T^{-1}$ );
- $\bar{u}$  = mean flow velocity, ( $L T^{-1}$ );
- $\bar{u}_a$  = effective velocity of bed-load particles, ( $L T^{-1}$ );
- $u'$  = longitudinal flow velocity fluctuation, ( $L T^{-1}$ );
- $u_b$  = transport velocity of bed-load particles, ( $L T^{-1}$ );
- $u_*$  = overall bed-shear velocity, ( $L T^{-1}$ );
- $u'_*$  = bed-shear velocity related to grains, ( $L T^{-1}$ );
- $u_{*,cr}$  = critical bed-shear velocity for initiation of motion, ( $L T^{-1}$ );
- $u_{*,crs}$  = critical bed-shear velocity for initiation of suspension, ( $L T^{-1}$ );
- $w$  = local mean vertical flow velocity, ( $L T^{-1}$ );
- $w'$  = vertical flow velocity fluctuation, ( $L T^{-1}$ );
- $w_s$  = particle fall velocity in clear still fluid, ( $L T^{-1}$ );
- $w_{s,m}$  = particle velocity in sediment-fluid mixture, ( $L T^{-1}$ );
- $Z, Z'$  = suspension number;
- $z$  = vertical coordinate, (L);
- $z_0$  = zero velocity level, (L);

$\beta$	=	ratio of sediment diffusion and fluid diffusion coefficient;
$\Delta$	=	bed form height, (L);
$\delta_b$	=	saltation height, (L);
$\epsilon_f$	=	diffusion coefficient of fluid, ( $L^2 T^{-1}$ );
$\epsilon_m$	=	diffusion coefficient of sediment, ( $L^2 T^{-1}$ );
$\epsilon_s$	=	diffusion coefficient of sediment, ( $L^2 T^{-1}$ );
$\kappa$	=	constant of Von Karman for clear fluid;
$\kappa_m$	=	constant of Von Karman for fluid-sediment mixture;
$\lambda$	=	bed form length, (L);
$\mu$	=	dynamic viscosity coefficient, ( $ML^{-1} T^{-1}$ );
$\mu_b$	=	bed form factor;
$\nu$	=	kinematic viscosity coefficient for clear fluid, ( $L^2 T^{-1}$ );
$\nu_m$	=	kinematic viscosity coefficient for a fluid-sediment mixture, ( $L^2 T^{-1}$ );
$\rho$	=	density of fluid, ( $ML^{-3}$ );
$\rho_s$	=	density of sediment, ( $ML^{-3}$ );
$\sigma_s$	=	geometric standard deviation of bed material;
$\tau$	=	shear stress, ( $ML^{-1} T^{-2}$ );
$\phi$	=	ratio of diffusion coefficient in fluid-sediment mixture and clear fluid; and
$\varphi$	=	correction factor for concentration profile.